Journal of Applied Physics ARTICLE pubs.aip.org/aip/jap

Wurtzite vs zinc blende phase selection in GaN nanowires

Cite as: J. Appl. Phys. **138**, 035304 (2025); doi: 10.1063/5.0279475
Submitted: 7 May 2025 · Accepted: 26 June 2025 ·
Published Online: 21 July 2025

Corentin Guérin,[1,a)] Fabien Jourdan,[1] Bérangère Moreau,[2] Bruno Gayral,[1] Jean-Luc Rouvière,[2] Gwénolé Jacopin,[3] and Bruno Daudin[1,b)]

AFFILIATIONS

[1]Univ. Grenoble Alpes, Grenoble INP, CEA, IRIG, PHELIQS, NPSC, 17 av. des Martyrs, 38000 Grenoble, France
[2]Univ. Grenoble Alpes, Grenoble INP, CEA, IRIG, MEM, LEMMA, 17 av. des Martyrs, 38000 Grenoble, France
[3]Univ. Grenoble Alpes, CNRS, Grenoble INP, Institut Néel, 38000 Grenoble, France

[a)]**Author to whom correspondence should be addressed:** corentin.guerin@cea.fr
[b)]**E-mail:** bruno.daudin@cea.fr

ABSTRACT

Due to the difference between the bandgap value of wurtzite and zincblende GaN variants, the realization of homo-epitaxial wurtzite/zinc-blende GaN heterostructures has been considered for long as an attractive possibility to grow optoelectronic devices exhibiting a reduced internal electric field. In accordance with this goal, we show that controlled phase selection can be achieved in GaN nanowire heterostructures, taking advantage of the absence of extended defects acting as extrinsic nucleation centers. Zinc blende GaN nanowire sections were grown in the Ga-rich regime at low temperatures while wurtzite sections were grown at high temperatures in slightly N-rich conditions. High resolution scanning electron microscopy experiments demonstrate atomically flat interfaces, opening the path to the realization of homo-epitaxial optoelectronic devices emitting in the UV-A wavelength range.

INTRODUCTION

Due to the 200 meV bandgap difference between wurtzite (WZ) and zinc blende (ZB) GaN polytypes, the possibility to realize homo-epitaxial WZ/ZB heterostructures for light emitting devices in the UV-A wavelength range has been identified for long. In particular, it was shown that basal stacking faults (SFs) in GaN, which consist of a deviation from regular wurtzite (WZ) ABABAB (0001) plane stacking into zinc blende (ZB) ABCABC (111) plane stacking, indeed, behave as ultrathin quantum wells (QWs) opening the path to the realization of such devices.[1–3] However, wavelength emission tuning through carrier confinement is hindered by the difficulty to control the growth of arbitrarily thick pure ZB GaN layers due to the higher thermodynamical stability of the WZ phase. In practice, when aiming at growing ZB GaN, uncontrolled WZ/ZB crystallographic phase mixing is often observed, associated with the presence of defects in layers triggering nucleation of the more stable WZ variant.[4,5] On the contrary, realization of practical homo-epitaxial devices requires a controlled conversion at the monolayer (ML) scale from WZ to ZB and vice versa, which has not been achieved to date.

Nanowires (NWs), which are nanocrystals free of extended defects, provide a new paradigm to overcome the above difficulty. In the case of catalyst-grown NWs, which are prone to exhibit polytypism, the controlled formation of ZB and WZ sections is achieved by controlling the size and the wetting angle of the catalyst droplet.[6] This approach does not hold in the case of GaN NWs, which are grown catalyst-free in plasma-assisted molecular beam epitaxy (PA-MBE). Nevertheless, it will be shown that it is possible to kinetically control the crystallographic variant, either ZB or WZ, and realize ZB insertions of controlled thickness and atomically flat interfaces in WZ GaN NWs. This is achieved by selecting an appropriate growth temperature and a Ga/N flux ratio. Using a combination of high resolution scanning electron microscopy (HR-STEM), photoluminescence (PL), and cathodoluminescence (CL) experiments, the structural and optical properties of the ZB/WZ GaN NW heterostructures will be discussed, emphasizing the key role of kinetics.

RESULTS AND DISCUSSION

The samples were grown by plasma-assisted molecular beam epitaxy (PA-MBE). The substrates consisted of regularly spaced GaN pillars grown by metalorganic chemical vapor deposition on a patterned Si substrate.[7] After introduction in the MBE growth chamber and outgassing at 350 °C during 2 h, an additional NW section was grown on top of the WZ GaN pillar substrate. In sample A, a first GaN section was grown at $T_S = 825$ °C during 30 min with a III/V ratio of 2, corresponding to a length of about 150 nm. It was found in this case that GaN NWs exhibited WZ phase with [1−102] facets, assessed by RHEED, typical of N-rich conditions. Next, temperature was continuously decreased down to 730 °C, without changing the Ga and N fluxes while pursuing growth during 30 min, which corresponded to an estimated length of about 200 nm. As a consequence of the decrease in Ga desorption associated with lower T_S, the Ga/active N flux ratio value evolved from N-rich to Ga-rich, eventually resulting in excess Ga accumulation on the substrate base plane and Ga droplet formation. As the NW growth mechanism is dominated by adatom diffusion from the basal plane toward the NWs and next along the sidewalls to the top surface,[8] Ga accumulation locally resulted in very Ga-rich conditions. After growth, this Ga excess on the NW top was removed by dipping in HCl. The effect of local accumulation of Ga on the substrate on the morphology of the top GaN NW section is illustrated in Fig. 1. In particular, it appears that NWs grown in the droplet region are well separated from each other, whereas NWs out from the droplet region are wider and tend to coalesce.

To analyze the influence of Ga droplet on the NW growth, we performed cathodoluminescence (CL) spectroscopy at T = 300 K. The acceleration voltage has been set to 5 kV to only probe the MBE regrown section, while the probe current was around 1 nA. Figure 1(a) shows the CL spectra acquired on and outside the Ga droplet. Outside the Ga droplet region, the main emission is centered at 3.42 eV, which corresponds to the luminescence of WZ GaN near band edge (NBE) emission.[9] In the Ga droplet region, the luminescence is dominated by an emission centered around 3.18 eV, which corresponds to the luminescence of ZB NBE.[10] Notably, it is worth noting that CL emission from the ZB region is 15–20 times more intense compared to the region dominated by WZ emission. The influence of the Ga droplet on growth is confirmed by panchromatic images acquired at 3.20 ± 0.04 eV [Fig. 1(b)] and at 3.40 ± 0.04 eV [Fig. 1(c)]. Indeed, the emission associated with the ZB phase comes only from the Ga droplet region, while WZ emission rather comes from outside the Ga droplet. It is concluded that Ga-rich growth conditions and relatively low T_S are resulting in ZB GaN NW formation, consistent with previous observations in the case of layers.[11,12]

In the next step, taking advantage of the above findings, sample B was grown at 650 °C, using a nominal Ga/N flux ratio of 1.6. Growth duration was 30 min, corresponding to a length of 250 nm. Scanning electron microscopy (SEM) images in Figs. 2(a)–2(d) put in evidence a polyhedral structure of the top GaN NW section, which is assigned to ZB crystallographic variant. This is further confirmed by low temperature PL measurements, using a laser excitation at 244 nm. The spot size was 30 μm, corresponding to about 4300 NWs. The beam makes an angle of 30° with the normal of the sample. Experiments were performed in four different spots separated from about 1 mm, to rule out the effect of temperature gradient over the sample. The results are shown in Fig. 2(e). WZ near the band edge (NBE) comes, at least, partly from the pedestal substrate. The ZB contribution at 3.269 eV, with a faint high energy shoulder at about 3.275 eV is dominant for the four analyzed spots, assessing the presence of strain relaxed GaN in the ZB phase all over the sample.[13] The peak at 3.160 eV is assigned to DAP contribution of ZB GaN, accompanied at a lower energy by 1LO phonon replica.[10,14] No stacking fault (SF) optical signature is visible between ZB and WZ NBE emission peaks.

High resolution scanning transmission electron microscopy (HR-STEM) observations were performed on a focused ion beam (FIB) prepared lamella from sample B. 4K × 4K HR-STEM images were taken along the [2−1−10] zone axis on a TITAN Themis microscope at 200 kV. By using a low magnification of about ×200 K, it was possible to acquire a large field of view of about

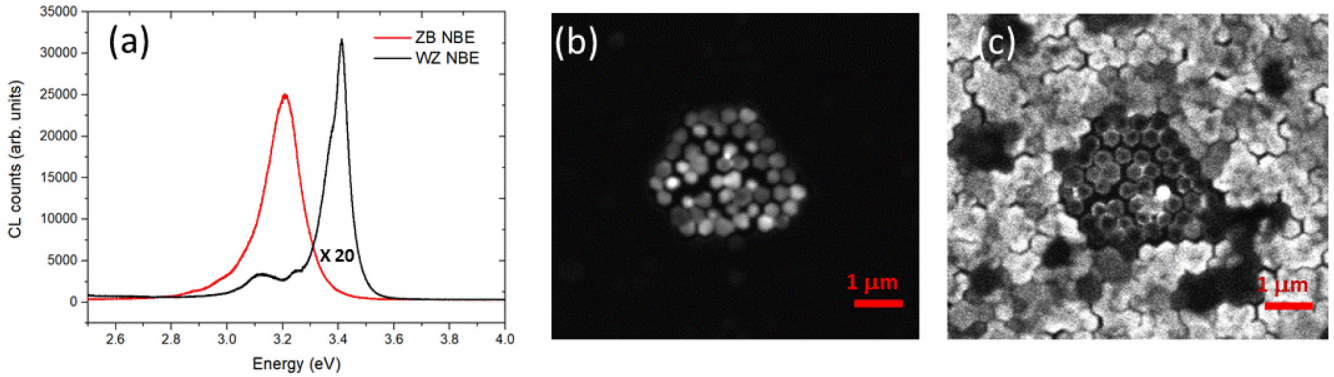

FIG. 1. (a) CL spectra in ZB and WZ areas at 300 K. (b) Panchromatic CL mapping of sample A acquired at 3.2 ± 0.04 eV, corresponding to ZB GaN, (c) mapping at 3.4 ± 0.04 eV, corresponding to WZ GaN.

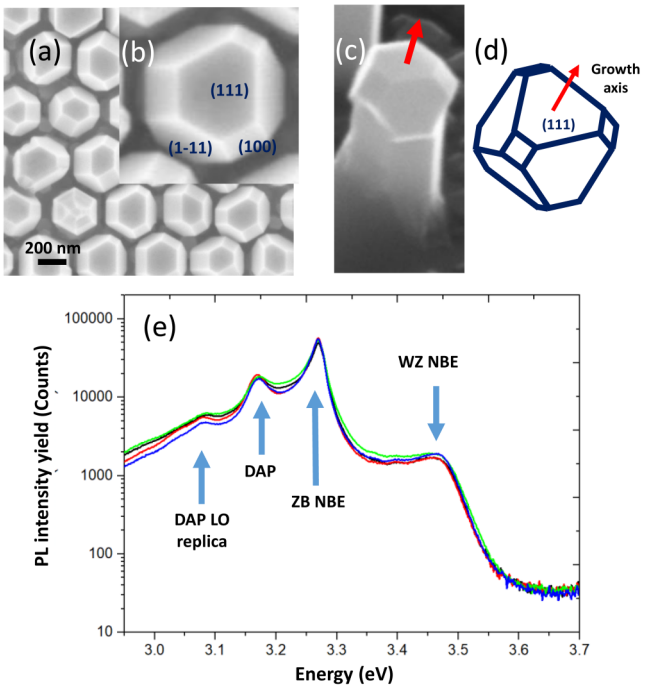

FIG. 2. (a) SEM image of an ensemble of cubic GaN nanowires. (b) and (c) Top view and bird view zoom on a single NW: the three types of facets are consistent with (d) natural facets of the cube. Growth axis is (111), parallel to the (0001) wurtzite axis of the pedestal substrate. (e) 5 K PL spectra in four different spots on the ensemble of ZB GaN NWs.

500 nm while preserving atomic scale information, as shown in Fig. 3(a). The overall length of the MBE grown section on the MOCVD pedestal is about 200 nm, consistent with the expected nominal length. As can be seen in the Fourier transform in Fig. 3(b), the (0002) and (101) atomic planes of, respectively, WZ and ZB have a periodicity of about 2 pixels, i.e., close to the Nyquist limit, and atomic planes are, in fact, hardly seen by the naked eye. Geometrical phase analysis (GPA) was used to extract structural information from these "Near-Nyquist-HR-STEM" images to identify the location of the different phases and evaluate the strain and defects possibly present in the structure. The GPA technique was first reported by Takeda *et al.*[15] and Hÿtch *et al.*[16] Later, Rouvière *et al.*[17] pointed out the interest and simplicity of performing a 1D-GPA analysis. In 1D-GPA analysis, as in the first step of the classical 2D-GPA analysis, one family of crystallographic plane g is selected by introducing a mask in the Fourier transform of the image. From this unique "g" frequency selection, GPA consists of computing the associated g-amplitude, g-phase, and g-Moiré images. The g-Moiré image is a special display of the g-phase information giving a visual representation of strain and detecting the presence of possible defects such as edge dislocations and stacking fault.[18,19] A HR-STEM image of a single NW is shown in Fig. 3(a). By choosing the crystallographic planes corresponding to either the ZB or WZ phase or common to both phases in the Fourier transform of the HR image [see Fig. 3(b)], amplitude images in Figs. 3(c)–3(e) were obtained, putting in evidence the sharp interface between WZ GaN pedestal and ZB upper part. The dark lines in Figs. 3(c) and 3(e) correspond to a SF initiating at the WZ/ZB interface, as shown in the g-Moiré image in Fig. 3(f) using the common g = (000−2)WZ/(−11−1)ZB spot [red spot in Fig. 2(b)].

Sample C was then grown, with the purpose of demonstrating the reverse transition from ZB GaN toward WZ. Once the ZB section, about 100 nm thick, has been completed using the same growth conditions as for the ZB section of sample B, both Ga and N cells were shuttered and the sample rapidly heated at 780 °C to desorb Ga excess. Next, growth was resumed using a Ga/N flux ratio equal to 0.8 and temperature set at 750 °C in order to grow a 200 nm thick GaN upper section. The results are shown in Figs. 4(a)–4(c), where the SEM image of a single NW exhibits the characteristic polyhedral top as well as CL mapping at 3.40 and 3.26 eV corresponding to both WZ and ZB band edges, respectively. The HR-STEM image of one NW is shown in Fig. 4(d). GPA amplitude images corresponding to the WZ and ZB phases are shown in Figs. 4(e) and 4(f), respectively. Interestingly, a stacking fault (SF) is visible in the ZB section, starting and finishing at the atomically flat c-plane interface between both crystallographic phases. CL at both room and low temperatures is shown in Fig. 4(g), dominated by the near band edge contribution of the ZB and WZ sections. As previously shown in Fig. 2, the peak at 3.16 eV in the low temperature spectrum is assigned to DAP contribution, with the associated 1LO and 2LO phonon replica.[10,14] Also, a faint peak is observed around 3.35 eV, which is tentatively assigned to the presence of WZ SFs in the ZB section.[20]

The submonolayer nucleation of GaN homoepitaxially grown on GaN was recently investigated by Peng Su *et al.*[21] They established that submonolayer growth occurs through the formation of triangular nuclei. In the absence of extrinsic nucleation centers such as dislocations or grain boundaries, the size and density of such nuclei are governed by both atomic fluxes and temperature. Accordingly, in the case of NWs exhibiting a diameter in the 200–300 nm range and in the absence of extended defects acting as extrinsic nucleation centers, it is expected that submonolayer growth will be dominated by diffusion and nucleation kinetics.

On the one hand, Ga adatom diffusion was theoretically investigated by Zywietz *et al.*[22] In particular, it was found that the WZ and ZB Ga adsorption sites on (0001) GaN were energetically similar in Ga-rich growth conditions, Ga migration from one site to another being governed by a diffusion barrier equal to 0.4 eV and a large Ga mobility. In addition, the presence of Ga in excess on the surface favors N capture by Ga adatoms to the expense of their recombination followed by N_2 molecule desorption.[22] It is worth pointing out that in such conditions, Ga adatom diffusion length may be of the order of the NW diameter, suggesting the occurrence of a single nucleation event per monolayer.[23]

On the other hand, Zang *et al.* recently investigated the competition between ZB and WZ phases in the nucleation stage.[24] These authors pointed out that small ZB phase GaN nuclei are, indeed, energetically favorable, despite the higher thermodynamical stability of the WZ phase with respect to its ZB counterpart. In accordance with these results, we propose that ZB phase formation

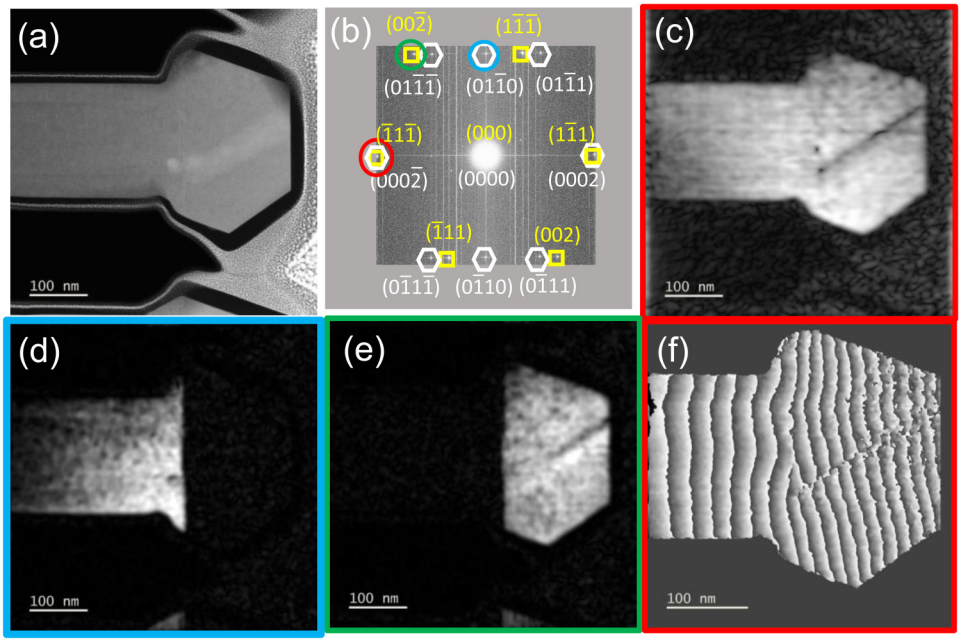

FIG. 3. (a) 4K × 4K near-Nyquist-HR-STEM image of a single NW (b) Fourier transform of image (a), showing the diffraction spots corresponding to ZB (yellow squares) and WZ (white hexagons), respectively. (c)–(e) g-amplitude images obtained by selecting circular masks with different g-planes. In (c), the red mask in (b) selects both the g = (000−2) planes of WZ and the g = (−1,1,−1) planes of ZB. In (d), the blue mask in (b) selects only the g = (0,1,−10) planes of WZ. In (e), the green mask in (b) selects only the g = (0,0,−2) planes of ZB. (f) g-moiré images obtained by using the red mask in (b) as in (c). In order to have more pixels per crystallographic plane, the starting HR-STEM image of (f) has a magnification 1.5 times higher than the one in (a). The black line in (c) corresponds to a stacking fault initiating at the WZ/ZB interface, as put in evidence in (f) the moiré image.

at low temperature results from the saturation of all available Ga adsorption sites on the surface in Ga-rich conditions, which favors the formation of ZB phase nuclei to the expense of WZ ones in a process dominated by nucleation kinetics rather than by Ga adatom diffusion.[25] As predicted by Zang *et al.*, the coordination properties of the initial ZB nucleus are maintained during its expansion process till completion of a full ZB ML.[24] Repetition of this process leads to the formation of a ZB GaN NW section, with an abrupt interface with the WZ GaN base. Conversely, when shifting to high growth temperature and a Ga/N ratio of about 0.8, i.e., in N-rich conditions, the WZ-coordinated Ga site turns to be energetically more favorable than its ZB-coordinated counterpart.[22] In such conditions, at temperatures high enough to ensure sufficient Ga adatom diffusion, high N coverage favors the formation and

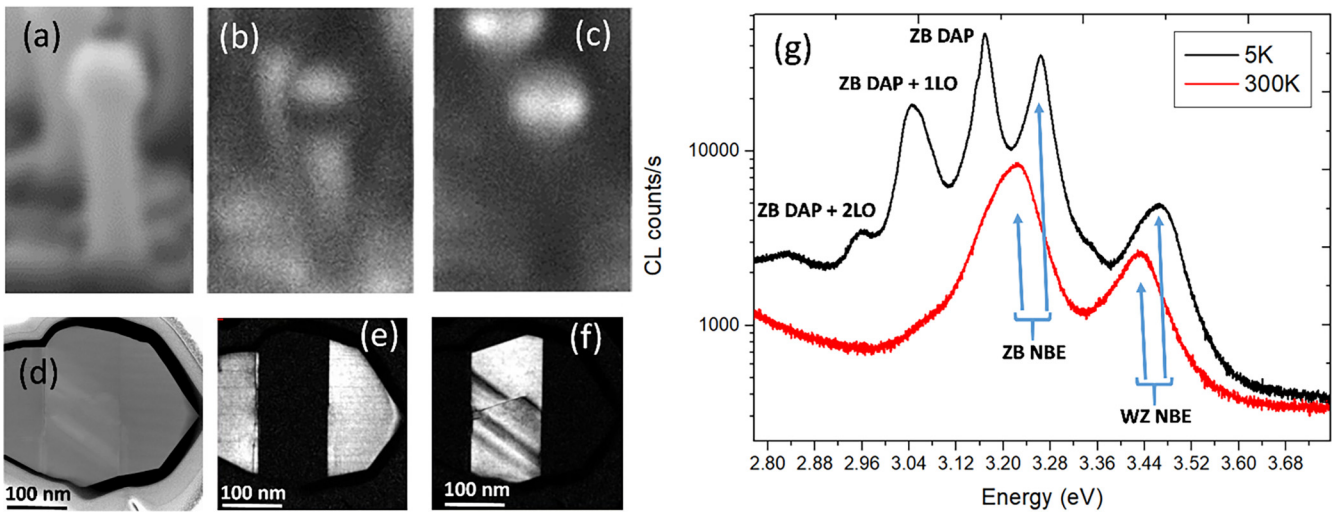

FIG. 4. (a) SEM image of a single ZB/WZ GaN NW in the CL setup. (b) CL mapping (at 300 K) at 3.4 eV, corresponding to the WZ phase. (c) CL mapping (at 300 K) at 3.26 eV, corresponding to the ZB phase. (d) HR-STEM image of a single NW. (e) GPA amplitude image corresponding to WZ. (f) GPA amplitude image corresponding to ZB. One SF initiating at the WZ/ZB interface is visible. (g) PL spectra of an ensemble of ZB/WZ GaN NWs.

stabilization of the thermodynamically more stable WZ phase in a process dominated by Ga adatom diffusion.[25] However, the absence of antiphase domains in the HR-STEM data, further suggests that the growth of each new layer on top of the NW obeys a mononuclear regime; also, in this case, discarding the occurrence of competition between different domains randomly nucleated. Interestingly, an abrupt ZB/WZ GaN interface is observed in the basal plane, a result specific to the NWs that we assign to the absence of extended defects acting as parasitic nucleation centers in layers.

At this stage, it has to be stressed that the process governing ZB GaN NW segment formation reported here is drastically different from ZB SF formation in WZ GaN. Indeed, in (0001) GaN layers, SF formation is observed at low temperatures and N-rich conditions, i.e., for the N-terminated surface. These conditions correspond to a large Ga adatom diffusion barrier, which results in the random trapping of Ga adatoms in unfavorable ZB sites and the eventual formation of a ZB nucleus.[22] By contrast, ZB GaN formation under Ga-rich conditions is triggered by nucleation kinetics, further emphasizing the different nature of the diffusion-limited and kinetically-limited GaN growth regimes.[25]

CONCLUSION

In conclusion, we have shown that the alternated growth of the ZB and WZ GaN NW sections can be controlled by an appropriate choice of growth conditions, emphasizing the role of nucleation kinetics. Remarkably, the ZB/WZ and WZ/ZB interfaces were found to be atomically flat. This opens the path to the realization of homo-epitaxial UV-A light emitting devices, free of misfit dislocations. Such heterostructures are furthermore expected to exhibit a reduced quantum confined Stark effect due to the absence of piezoelectric polarization contribution to the total internal electric field and should, therefore, exhibit higher emission intensity at saturation and less power dependent wavelength shift than ternary alloy-based heterostructures emitting in the same wavelength range.

ACKNOWLEDGMENTS

The authors acknowledge support from the French ANR agency (Project ANABASE, No. ANR-22-CE09-0031). They also acknowledge support from GANEXT (No. ANR-11-LABX-0014). GANEXT belongs to the public funded "Investissements d'Avenir" program managed by the French ANR agency. The authors thank Fabrice Donatini for his help with cathodoluminescence measurements.

AUTHOR DECLARATIONS

Conflict of Interest

The authors have no conflicts to disclose.

Author Contributions

Corentin Guérin: Data curation (equal); Formal analysis (equal); Investigation (equal); Methodology (equal); Software (equal); Validation (equal); Writing – review & editing (equal). **Fabien Jourdan:** Data curation (equal); Formal analysis (equal); Investigation (equal); Methodology (equal); Resources (equal); Software (equal); Visualization (equal). **Bérangère Moreau:** Resources (equal). **Bruno Gayral:** Methodology (equal); Resources (equal); Validation (equal); Writing – review & editing (equal). **Jean-Luc Rouvière:** Data curation (equal); Investigation (equal); Methodology (equal); Resources (equal); Software (equal); Validation (equal); Visualization (equal). **Gwénolé Jacopin:** Supervision (supporting); Validation (equal); Writing – review & editing (equal). **Bruno Daudin:** Conceptualization (equal); Formal analysis (equal); Funding acquisition (equal); Investigation (equal); Methodology (equal); Project administration (equal); Supervision (equal); Validation (equal); Visualization (equal); Writing – original draft (equal); Writing – review & editing (equal).

DATA AVAILABILITY

The data that support the findings of this study are available within the article.

REFERENCES

[1]W. Rieger, R. Dimitrov, D. Brunner, E. Rohrer, O. Ambacher, and M. Stutzmann, "Defect-related optical transitions in GaN," Phys. Rev. B **54**, 17596 (1996).
[2]M. Albrecht, S. Christiansen, G. Salviati, C. Zanotti-Fregonara, Y. T. Rebane, Y. G. Shreter, M. Mayer, A. Pelzmann, M. Kamp, K. J. Ebeling, M. D. Bremser, R. F. Davis, and H. P. Strunk, "Luminescence related to stacking faults in heteroepitaxially grown Wurtzite GaN," MRS Proc. **468**(1), 293–298 (1997).
[3]C. Stampfl and C. G. Van de Walle, "Energetics and electronic structure of stacking faults in AlN, GaN, and InN," Phys. Rev. B **57**, R15052 (1998).
[4]J. W. Yang, J. N. Kuznia, Q. C. Chen, M. Asif Khan, T. George, M. De Graef, and S. Mahajan, "Temperature-mediated phase selection during growth of GaN on (111)A and (1¯1¯1¯)B GaAs substrates," Appl. Phys. Lett. **67**, 3759 (1995).
[5]E. Martinez-Guerrero, E. Bellet-Amalric, L. Martinet, G. Feuillet, B. Daudin, H. Mariette, P. Holliger, C. Dubois, C. Bru-Chevallier, P. Aboughe Nze, T. Chassagne, G. Ferro, and Y. Monteil, "Structural properties of undoped and doped cubic GaN grown on SiC (001)," J. Appl. Phys. **91**, 4983 (2002).
[6]F. Panciera, Z. Baraissov, G. Patriarche, V. G. Dubrovskii, F. Glas, L. Travers, U. Mirsaidov, and J.-C. Harmand, "Phase selection in self-catalyzed GaAs nanowires," Nano Lett. **20**, 1669 (2020).
[7]C. Guérin, F. Jourdan, G. Jacopin, and B. Daudin, "Growth and optical characterization of in-plane-ordered AlN nanowires for UV−C emitting devices," ACS Appl. Nano Mater. **7**, 20301 (2024).
[8]R. Songmuang, T. Ben, B. Daudin, D. González, and E. Monroy, "Identification of III–N nanowire growth kinetics via a marker technique," Nanotechnology **21**, 295605 (2010).
[9]B. Monemar, "Fundamental energy gap of GaN from photoluminescence excitation spectra," Phys. Rev. B **10**, 676 (1974).
[10]D. J. As, F. Schmilgus, C. Wang, B. Schöttker, D. Schikora, and K. Lischka, "The near band edge photoluminescence of cubic GaN epilayers," Appl. Phys. Lett. **70**, 1311 (1997).
[11]H. Okumura, K. Balakrishnan, H. Hamaguchi, T. Koizumi, S. Chichibu, H. Nakanishi, T. Nagatomo, and S. Yoshida, "Analysis of MBE growth mode for GaN epilayers by RHEED," J. Cryst. Growth **189–190**, 364 (1998).
[12]B. M. Shi, M. H. Xie, H. S. Wu, N. Wang, and S. Y. Tong, "Transition between wurtzite and zinc-blende GaN: An effect of deposition condition of molecular-beam epitaxy," Appl. Phys. Lett. **89**, 151921 (2006).
[13]J. Renard, G. Tourbot, D. Sam-Giao, C. Bougerol, B. Daudin, and B. Gayral, "Optical spectroscopy of cubic GaN in nanowires," Appl. Phys. Lett. **97**, 081910 (2010).

[14]Z. X. Liu, A. R. Goñi, K. Syassen, H. Siegle, C. Thomsen, B. Schöttker, D. J. As, and D. Schikora, "Pressure and temperature effects on optical transitions in cubic GaN," J. Appl. Phys. **86**, 929 (1999).
[15]M. Takeda and J. Suzuki, "Crystallographic heterodyne phase detection for highly sensitive lattice-distortion measurements," J. Opt. Soc. Am. A **13**, 1495 (1996).
[16]M. J. Hÿtch, E. Snoeck, and R. Kilaas, "Quantitative measurement of displacement and strain fields from HREM micrographs," Ultramicroscopy **74**, 131 (1998).
[17]J. L. Rouvière and E. Sarigiannidou, "Theoretical discussions on the geometrical phase analysis," Ultramicroscopy **106**, 1 (2005).
[18]A. M. N. Quach, N. Rochat, J.-L. Rouvière, J. Napierala, and B. Daudin, "Non-radiative recombination centres in InGaN/GaN nanowires revealed by statistical analysis of cathodoluminescence intensity maps and electron microscopy," Nanotechnology **35**, 495706 (2024).
[19]N. Chaize, X. Baudry, P.-H. Jouneau, E. Gautier, J.-L. Rouvière, Y. Deblock, J. Xu, M. Berthe, C. Barbot, B. Grandidier, L. Desplanque, H. Sellier, and P. Ballet, "Selective area epitaxy of in-plane HgTe nanostructures on CdTe(001) substrate," Nanotechnology **35**, 505602 (2024).
[20]S. A. Church, S. Hammersley, P. W. Mitchell, M. J. Kappers, L. Y. Lee, F. Massabuau, S. L. Sahonta, M. Frentrup, L. J. Shaw, D. J. Wallis, C. J. Humphreys, R. A. Oliver, D. J. Binks, and P. Dawson, "Effect of stacking faults on the photoluminescence spectrum of zincblende GaN," J. Appl. Phys. **123**, 185705 (2018).
[21]P. Su, W. Ai, X. Chen, and L. Liu, "Microscopic study of submonolayer nucleation characteristics during GaN (0001) homoepitaxial growth," J. Vac. Sci. Technol. A **41**, 062704 (2023).
[22]T. Zywietz, J. Neugebauer, and M. Scheffler, "Adatom diffusion at GaN (0001) and (0001¯) surfaces," Appl. Phys. Lett. **73**, 487 (1998).
[23]M. Gruart, G. Jacopin, and B. Daudin, "Role of Ga surface diffusion in the elongation mechanism and optical properties of catalyst-free GaN nanowires grown by molecular beam epitaxy," Nano Lett. **19**, 4250 (2019).
[24]H. Zang, Z. Shi, J. Ben, K. Jiang, Y. Chen, S. Zhang, M. Liu, T. Wu, Y. Jia, X. Sun, and D. Li, "Growth mechanism and electronic properties of stacking mismatch boundaries in wurtzite III-nitride material," Phys. Rev B **107**, 165308 (2023).
[25]M. H. Xie, M. Gong, E. K. Y. Pang, H. S. Wu, and S. Y. Tong, "Origin of triangular island shape and double-step bunching during GaN growth by molecular-beam epitaxy under excess Ga conditions," Phys. Rev B **74**, 085314 (2006).